Highly Photoconductive CdSe Quantum-Dot Films: Influence of Capping Molecules and Film Preparation Procedure

ARTICLE *in* THE JOURNAL OF PHYSICAL CHEMISTRY C · FEBRUARY 2010

Impact Factor: 4.77 · DOI: 10.1021/jp9109546

7 AUTHORS, INCLUDING:

Ruben D. Abellon
Delft University of Technology
24 PUBLICATIONS **536** CITATIONS
SEE PROFILE

Tom J. Savenije
Delft University of Technology
124 PUBLICATIONS **2,991** CITATIONS
SEE PROFILE

Arjan J Houtepen
Delft University of Technology
68 PUBLICATIONS **1,459** CITATIONS
SEE PROFILE

Laurens D A Siebbeles
Delft University of Technology
249 PUBLICATIONS **7,180** CITATIONS
SEE PROFILE

Highly Photoconductive CdSe Quantum-Dot Films: Influence of Capping Molecules and Film Preparation Procedure

Elise Talgorn, Elli Moysidou, Ruben D. Abellon, Tom J. Savenije, Albert Goossens, Arjan J. Houtepen,* and Laurens D. A. Siebbeles*

Department of Chemical Engineering, Delft University of Technology, Julianalaan 136, 2628 BL Delft, The Netherlands

Received: November 18, 2009; Revised Manuscript Received: January 14, 2010

Highly photoconductive films of CdSe nanocrystals have been prepared by exchanging the original bulky ligands with 1,2-ethanedithiol (EDT) and 1,2-ethanediamine (EDA). Different methods to achieve this exchange, layer-by-layer (LbL) deposition and soaking of drop-casted films, have been compared in detail. Introduction of EDT and EDA by the soaking method results in a broadening of the optical absorption due to disorder in the film. In contrast, the width of the absorption features is unaffected in the LbL films, while the position of the first optical absorption peak is red-shifted by tens of millielectronvolts. The photoluminescence is completely quenched for the LbL films. These findings are characteristic for strong and homogeneous electronic coupling between the quantum dots (QDs) in the LbL films. The photoconductivity of these films was studied with the time-resolved microwave conductivity (TRMC) technique. With this electrodeless technique effects of electrode injection on charge transport are avoided, so that information about the intrinsic mobility of charge carriers is obtained. We find that in simple drop-casted films the conductivity is mainly imaginary and dominated by the polarizability of photogenerated excitons. When the orginal ligands are exchanged by soaking or by the LbL procedure, the conductivity becomes real and dominated by interparticle transport of free charge carriers. It is found that the product of the exciton dissociation yield and the charge carrier mobility is 4×10^{-3} $cm^2/(V\ s)$ in the LbL grown films with EDA capping molecules. This implies that a surprisingly high fraction of free carriers is generated or, alternatively, that the carrier mobility is higher than all previously reported mobility values for layers of CdSe QDs.

1. Introduction

Thin films of colloidal quantum dots (QDs) are of great promise for application in optoelectronic devices.[1,2] Tunability of the energy of the electronic levels, control over the photoluminescence color and yield, carrier multiplication, chemical flexibility, and solution processing are some of the many interesting properties of QDs.[3−7] The properties of a QD film depend on the individual characteristics of the QDs and on their mutual interactions. For optoelectronic applications the electronic coupling between QDs must be sufficient for efficient motion of charges from one QD to another.

Colloidal QD solutions are stabilized by a layer of bulky ligands on the QD surface. The ligands maintain the integrity of the QDs and passivate surface dangling bonds, which can act as traps for electrons and holes. In a thin film the bulky surface ligands impede interaction between QDs and consequently lead to a considerable barrier for charge transport. A general approach to improve the charge carrier mobility is to introduce smaller capping molecules, so that the electronic coupling between adjacent QDs becomes larger.[8−11] Increased electronic coupling will lead to charge delocalization over different QDs, which reduces the electron−hole Coulomb interaction and enhances the quantum yield for photogeneration of charges.

A relatively high charge mobility approaching 1 $cm^2/(V\ s)$ has been reported for thin film field-effect transistors (FETs) based on an array of PbSe QDs capped with small hydrazine (N_2H_4) molecules.[8] Terahertz photoconductance measurements on films of PbSe QDs with various small capping molecules revealed similar charge mobilities.[12] Conversely, for films of CdSe QDs with small surface ligands the highest electron mobilities reported to date are only on the order of 10^{-2} $cm^2/(V\ s)$.[9,13,14] The lower mobility for CdSe QD films can at least in part be due to the larger charge carrier effective mass, which lowers the tunneling rate between adjacent QDs.[15,16] In addition, the film preparation procedure affects the film morphology and consequently the charge carrier mobility. Soaking of a drop-casted or spin-casted QD film in a solution containing shorter capping molecules is a widely used technique for capping exchange.[8,12,13,17−21] However, the efficiency of capping exchange is limited by slow ligand diffusion through the film. Furthermore, this technique leads to cracks because a shorter interparticle distance reduces the volume of the film.[12,19] An alternative method, the layer-by-layer (LbL) growth technique, has recently allowed the realization of very conductive crack-free PbSe QD films.[11,22] In this approach, a substrate is dipped successively in a QD solution and a solution of capping molecules with two functional groups that can bind to two neighboring QDs. This operation is typically repeated tens of times, and ideally each QD layer grows on top of the previous one. Although it is not certain that cross-linking is achieved by the bifunctional ligands,[22] efficient capping exchange has been found to occur, and homogeneous, conductive films can be grown.

The aim of this work is to provide insight into the extent to which the photoconductance of a CdSe QD film can be enhanced

* Corresponding authors. E-mail: A.J.Houtepen@tudelft.nl (A.J.H), L.D.A. Siebbeles@tudelft.nl (L.D.A.S.).

10.1021/jp9109546
Published on Web 02/05/2010

by replacing the commonly used bulky surface ligands by small 1,2-ethanedithiol (EDT) or 1,2-ethanediamine (EDA) molecules. Since thiols are known to efficiently trap holes in CdSe QDs,[23] the use of these two ligands allows one to compare the contribution from electrons and holes to the charge transport. Results for films prepared by soaking and LbL methods are compared. The films were characterized by optical absorption and photoluminescence measurements. Photogeneration and decay of charges were studied with the time-resolved microwave conductivity (TRMC) technique.[24] To our knowledge, this is the first time that TRMC has been applied to the study of colloidal quantum dots. With this electrodeless technique, effects due to long-range disorder and electrode injection on charge transport are avoided, so that information about the intrinsic mobility of charge carriers is obtained. It is found that the product of the exciton dissociation yield and the charge carrier mobility is 4×10^{-3} cm^2/(V s) in the LbL grown films with EDA capping molecules. This implies that a surprisingly high fraction of free carriers is generated or, alternatively, that the carrier mobility is higher than previously reported mobility values for layers of CdSe QDs.

2. Experimental Section

All experiments were carried under N_2 atmosphere and anhydrous solvents were used.

2.1. QD Synthesis. CdSe QDs were synthesized following the "green" recipe of Talapin et al.[25] This synthesis results in QDs stabilized by a combination of tri-*n*-octylphosphine oxide (TOPO), hexadecylamine (HDA), and *n*-tetradecylphosphonic acid (TDPA) ligand molecules. The QDs were precipitated with methanol, filtered, and redispersed in toluene. After repeating the latter procedure three times, the QDs were dispersed in a 9:1 v/v chloroform/octane mixture for drop-casting or in choloroform for capping exchange in solution or LbL growth of a film.

2.2. Capping Exchange in Solution. The effect of the presence of amine or thiol groups on the surface of individual CdSe QDs in solution (i.e., in absence electronic coupling between QDs) was studied by introducing hexylamine or hexanethiol surface ligands. To this end, QDs with the original TOPO/HDA/TDPA ligands were dispersed in 10% vol hexanethiol or 10% vol hexylamine in chloroform. The quantum-dot-to-ligand-molecule ratio was 1/10 000. The QD concentration was determined from optical density measurement and using the molar extinction coefficient given in ref 26. The capping exchange was left to proceed for 1 day before characterization of the dispersions.

2.3. Film Preparation. For introduction of capping molecules by the soaking method, films were first prepared by drop-casting QDs with TOPO/HDA/TDPA ligands dissolved in chloroform/octane on a quartz plate. The films were left to dry for 2 h. For capping exchange the drop-casted films were soaked for 1 min in a 0.1% vol EDT solution in methanol or in a 1% vol EDA solution in methanol. The films were subsequently rinsed with methanol to remove excess capping molecules. Longer soaking times or a higher concentration of capping molecules led to severe mechanical damage (the film crumbled).

The LbL growth procedure was carried out by dipping quartz substrates successively into the QD solution (with an optical density of 1.7 at the first exciton peak), a solution of EDT or EDA, and a rinsing solvent. The capping molecule solutions were 0.1% vol EDT in methanol or 10% vol EDA in methanol, and the rinsing solvent was methanol. The dipping time for each solution was 10 s for EDT and 1 min for EDA. Those dipping times were found to be sufficient for the film to grow. The longer dipping time for EDA is due to its weaker binding to the QD surface.[27] The dipping procedure was repeated 15 times. According to thickness measurements with a Veeco Dektak 8 step profilometer, each dipping cycle leads to deposition of one to two monolayers of QDs.

2.4. Optical Characterization. Optical absorption was measured using a Perkin-Elmer Lambda 900 spectrometer equipped with an integrating sphere. The optical density was measured and the attenuation F_a (fraction of incident photons that is absorbed by the sample) was obtained by correction for reflection losses. Photoluminescence spectra were measured with a Lifespec-ps setup (Edinburgh instrument) with a 405 nm excitation source.

2.5. Microwave Photoconductance Measurements. The photoconductance of QD films was measured using the time-resolved microwave conductivity (TRMC) technique. The TRMC setup has been described in detail previously.[24,28] Briefly, the samples were mounted in an X-band microwave cavity at a position of maximum electric field (100 V/cm). Upon photoexcitation the change in microwave power reflected from the cavity was measured. Photoexcitation laser pulses of 3 ns duration with a wavelength in the range 420−700 nm were obtained by pumping an optical parametric oscillator with the third harmonic of a Q-switched Nd:YAG laser. Pulses with a wavelength of 300 nm were produced by frequency-doubling the 600 nm pulse. The photon flux was varied between 10^{13} and 2×10^{15} photons/cm^2/pulse, using neutral density filters.

The change in reflected microwave power can be due to a change in the real or the imaginary component of the conductance of the sample.[29] Mobile charges that move with a velocity in phase with the oscillating microwave field give rise to a real conductance component. This real conductance leads to absorption of microwave power by the charge carriers. In the case of pure real conductance, the microwave power reflected from the cavity is reduced for all microwave frequencies, with the reduction being maximal at the resonance frequency of the cavity, as depicted in Figure 1A. The polarizibility of excitons leads to a change of the imaginary conductance and causes a phase shift of the microwaves. A purely imaginary conductance results in a shift of the resonance frequency of the cavity, as illustrated in Figure 1A.

For small photoinduced changes in the real conductance, $\Delta G(t)$, of the sample and negligible change in imaginary conductance, the relative change in microwave power is

$$\frac{\Delta P(t)}{P} = -K\Delta G(t) \tag{1}$$

In eq 1 the factor $\Delta P(t)/P = (P_{light}(t) - P_{dark})/P_{dark}$ with t being the time, P_{light} the reflected microwave power after laser excitation of the sample, and P_{dark} the reflected power without laser excitation. The sensitivity factor K depends on the dimensions and dielectric properties of the cavity and the sample and has been determined previously.[30] The real component of the photoconductance ΔG can be expressed as[28]

$$\Delta G(t) = e\beta I_o F_a \Phi(t) \sum \mu \tag{2}$$

where e is the elementary charge, β is the ratio between the broad and narrow inner dimensions of the waveguide, I_o is the photon fluence in the laser pulse, F_a is the fraction of light absorbed by the sample, $\Phi(t)$ is the quantum yield of generation

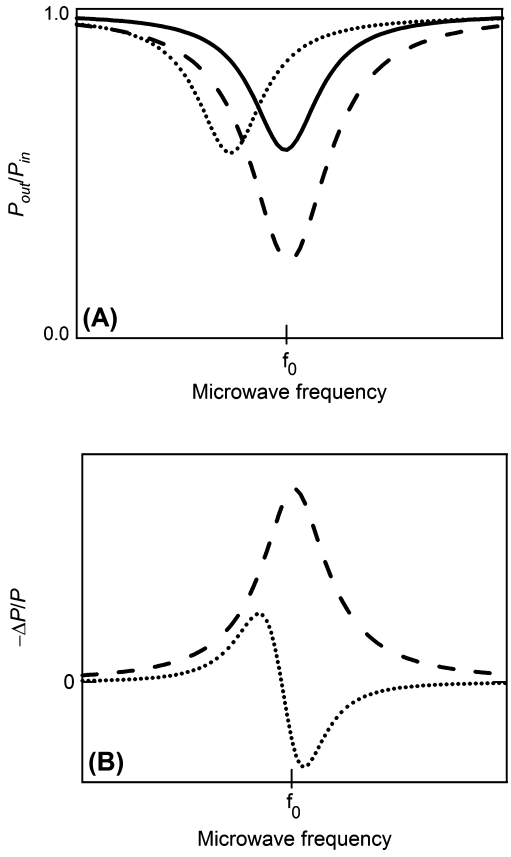

Figure 1. (A) Ratio of reflected microwave power, P_{out}, and incident power, P_{in}, versus microwave frequency in the absence of photoexcitation (full line) and after a photoinduced change in only the real (dashed line) and only the imaginary (dotted line) conductance. (B) Corresponding relative change in microwave power upon photoexcitation. The resonance frequency of the cavity loaded with the sample in the absence of photoexcitation is given by f_0.

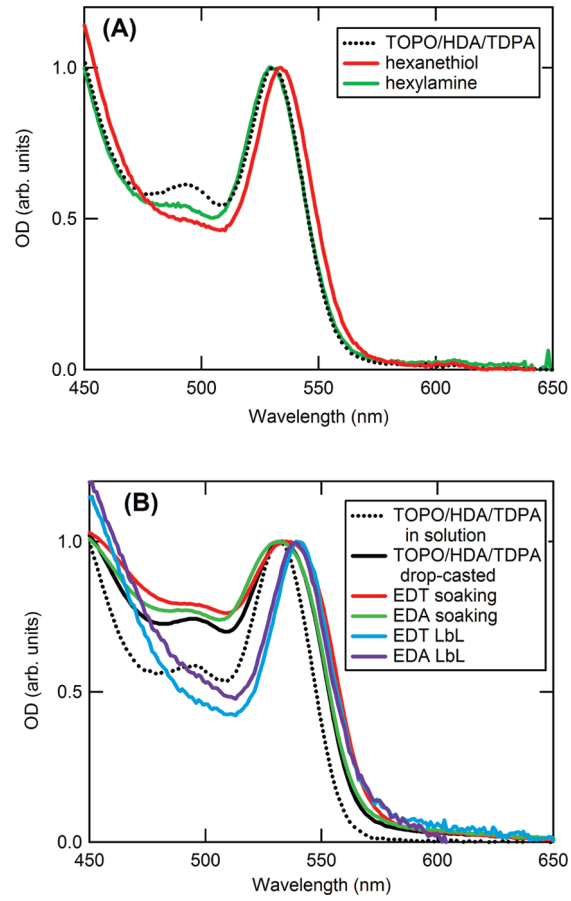

Figure 2. (A) Absorption spectra of solutions of QDs with TOPO/HDA/TDPA, hexanethiol, or hexylamine ligands. (B) Absorption spectrum of QDs with TOPO/HDA/TDPA ligands in solution and spectra of QD films. The spectra have been normalized to the magnitude of the first absorption peak.

of mobile charge carriers per absorbed photon at time t, and $\sum\mu$ is the sum of the electron and hole mobilities. After formation of mobile charge carriers by the laser pulse, the measured photoconductance increases on a time scale that is mainly determined by the 18 ns response time of the microwave cavity. The measured photoconductance reaches a maximum, ΔG_o, and subsequently decreases due to charge recombination and/or trapping. The product $\Phi_o\sum\mu$ is obtained from ΔG_o by use of eq 2. Since Φ_o is less than unity, the product $\Phi_o\sum\mu$ corresponds to the lower limit of $\sum\mu$.

3. Results and Discussion

3.1. Optical Characterization. Figure 2A shows the absorption spectra of the CdSe QDs in solution with the original bulky TOPO/HDA/TDPA ligands together with the spectra obtained after replacement of these ligands by hexanethiol or hexylamine molecules. Due to the presence of only one surface-binding group in the latter molecules, cross-linking and precipitation of the QDs are avoided and effects of electronic coupling between QDs are excluded. The spectra have been normalized to facilitate comparison of the position and width of the first absorption peak, which is due to the $1S_{3/2}1S_e$ electronic transition. The first absorption peak for CdSe QDs with TOPO/HDA/TDPA ligands is a maximum at 531 nm, which implies that the QD diameter is 2.8 nm.[31] Fit of a Gaussian function to the peak yields a full width at half-maximum (fwhm) of 19 nm.

Replacement of TOPO/HDA/TDPA ligands by hexanethiol molecules leads to a 3 nm (13 meV) red-shift of the first absorption maximum to 534 nm, while introduction of hexylamine molecules induces a 1 nm (4 meV) blue-shift to 530 nm; see Figure 2A. These shifts reflect that the nature of the surface binding groups of the ligand molecules determines the electronic interaction with the QD and affects the dielectric environment around the QD.[32]

Figure 2B shows the absorption spectra of the solution of CdSe QDs with TOPO/HDA/TDPA ligands together with spectra for different QD films. Drop-casting of QDs with TOPO/HDA/TDPA ligands leads to a 1 nm (4 meV) red-shift of the first absorption peak to 532 nm and a broadening by 5 nm to a fwhm of 24 nm, as compared with the QDs in solution. These effects are likely due to disorder in the QD film and possibly to some extent to electronic interaction between adjacent QDs in (parts of) the film. Soaking of the drop-casted film in EDT causes a red-shift of the first absorption peak to 534 nm, while soaking in EDA induces a blue-shift to 530 nm. These peak positions are identical to those for QDs with hexanethiol or hexylamine capping molecules in solution (see Figure 2A) and it thus appears that the peak position is mainly determined by interaction of the QDs with the capping molecules.

The first absorption peaks of the QD films with EDT or EDA capping molecules prepared via the LbL method appear at 540 nm and have a fwhm of 21 nm; see Figure 2B. The fwhm is only 2 nm larger than for the QDs in solution, which implies that disorder due to variations in local dielectric environment and/or varying electronic couplings between QDs is small. The absorption peak of the EDT LbL film is red-shifted by 6 nm

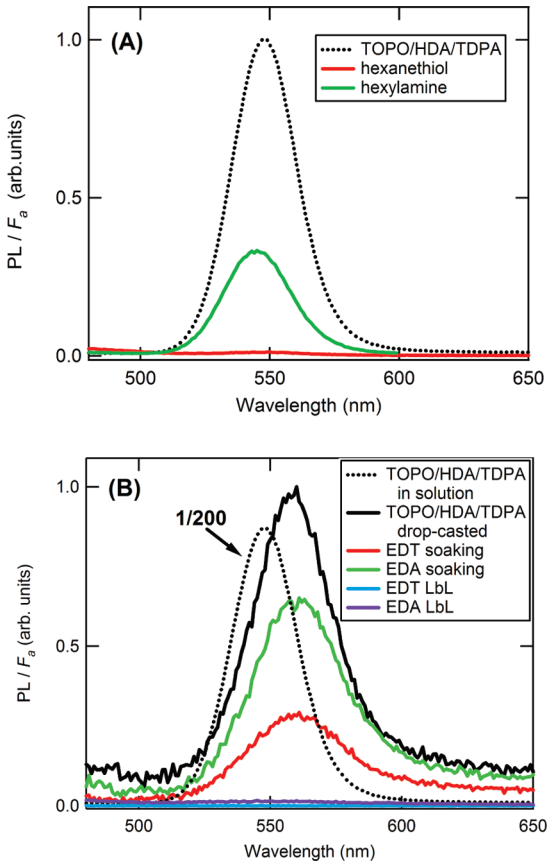

Figure 3. (A) Photoluminescence spectra of solutions of QDs with TOPO/HDA/TDPA, hexanethiol, or hexylamine ligands. (B) Photoluminescence spectrum of a solution of QDs with TOPO/HDA/TDPA ligands and spectra of QD films. The photoluminescence has been normalized to the fraction of absorbed photons. Note that the magnitude of the spectrum for QDs in solution in part B has been scaled by a factor of $^1/_{200}$.

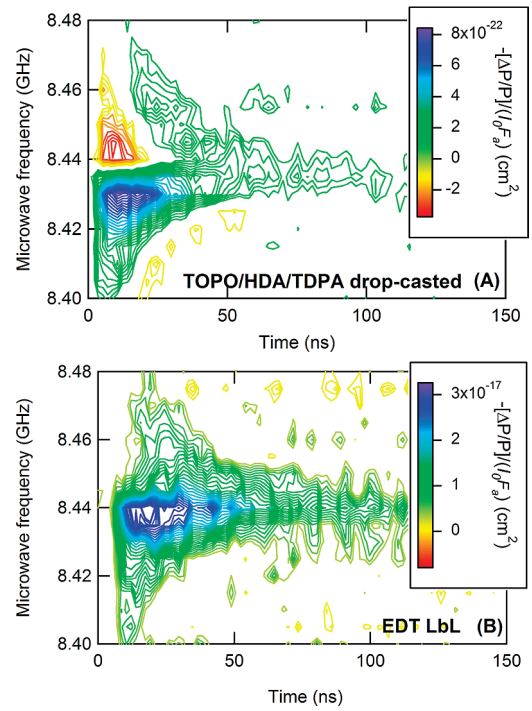

Figure 4. Relative change in microwave power as a function of microwave frequency and time upon photoexcitation of (A) the drop-casted QD film and (B) the EDT LbL film. The data have been normalized to the number of absorbed photons.

(26 meV), as compared with the solution of QDs with hexanethiol ligands in Figure 2A. The corresponding red-shift for the EDA LbL film is 10 nm (39 meV). These shifts can be attributed to electronic coupling between the QDs in the LbL grown films.[33]

Figure 3A shows the photoluminescence (PL) spectra normalized to the fraction of absorbed photons for QDs in solution. Replacement of the TOPO/HDA/TDPA ligands by hexanethiol molecules leads to complete PL quenching. The PL quenching can be attributed to hole transfer from the CdSe QDs to a thiol group in a hexanethiol molecule.[23,34] Introduction of hexylamine molecules causes the PL to decrease to a third of the value for QDs with TOPO/HDA/TDPA ligands. PL quenching of CdSe QDs upon addition of a large excess of amines has been reported.[35]

The PL spectra for the QD films are shown in Figure 3B, together with the spectrum for a solution of QDs with TOPO/HDA/TDPA ligands. Note, that the solution spectrum has been scaled by a factor $^1/_{200}$. The PL spectra for the drop-casted and soaked films are shifted by 13 nm (53 meV), as compared with the spectrum of QDs in solution. This red-shift is much larger than for the absorption (see Figure 2B) and can be attributed to exciton diffusion toward larger QDs within the size distribution, which luminesce at longer wavelength.[36] The data show that the PL efficiency for films is more than 2 orders of magnitude smaller than for the solution. This can be due to diffusional motion of excitons through the film, resulting in encounter of a quenching site where nonradiative decay occurs. Also, in a film photoexcitation can to a larger extent lead to generation of free electrons and holes that decay by nonradiative recombination. The PL efficiency of the soaked films is smaller than for the drop-casted film. However, the PL reduction for soaking with EDA and EDT is smaller than the PL reduction for capping exchange to amine or thiol ligands in solution (Figure 3A). This suggests that the soaking procedure results in a capping exchange that is far from complete.

The PL of the LbL grown films is completely quenched. This indicates that the capping exchange is much more efficient in the LbL grown films than it is in the soaked drop-casted films. For the LbL film with EDT capping molecules the PL quenching can be due to hole trapping by the thiol group. The complete PL quenching in the LbL film with EDA capping must be due to efficient exciton diffusion to quenching sites and/or photogeneration of free charges rather than excitons.

3.2. Microwave Photoconductance Measurements. Figure 4 shows the relative change in microwave power for the drop-casted film with TOPO/HDA/TDPA ligands and the EDT LbL film upon photoexcitation at the maximum of the first peak in the absorption spectrum; see Figure 2B. The data have been normalized to the number of photons absorbed by the film. At times shorter than 30 ns, the relative change in microwave power for the drop-casted film is positive (green/blue) below and negative (yellow/red) above the resonance frequency of the cavity (8.437 GHz); see Figure 4A. This clearly reflects a shift of the resonance frequency (see Figure 1), which implies that the photoconductance has a nonzero imaginary component. The fact that the positive signal below the resonance frequency is larger than the negative signal at higher frequency indicates that the photoconductance also has a nonzero real component. At times exceeding 30 ns the relative change of the microwave power is positive at all frequencies; see Figure 4A. As discussed in section 2.5, the real photoconductance (and negligible imaginary component) at longer times must be due to mobile

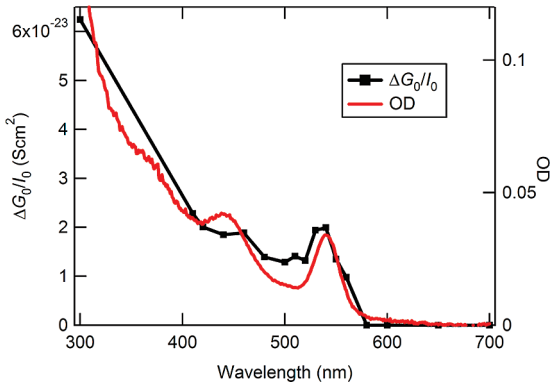

Figure 5. Photoaction spectrum (left-axis) and absorption spectrum (right-axis) for the EDT LbL film. The photoaction spectrum was obtained by using the same laser pump fluence for all wavelengths.

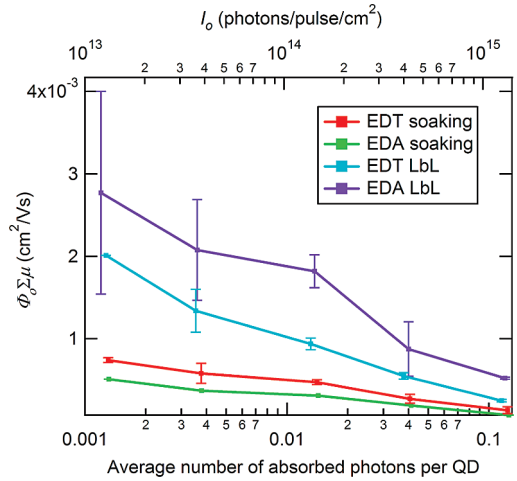

Figure 6. Effect of photoexcitation density on $\Phi_o\sum\mu$ for QD films that were prepared as indicated. The samples were photoexcited at the first absorption peak. The vertical bars represent the sample-to-sample variations.

charges that move in phase with the oscillating microwave field. The imaginary component at times shorter than 30 ns is attributed to the polarizability of excitons, as discussed in section 2.5. The picture that emerges from the above is that photoexcitation of the drop-casted film leads to generation of excitons that decay within 30 ns, in addition to formation of charges with a longer lifetime. Use of eqs 1 and 2 and fitting a single exponential decay of the real photoconductance after 40 ns followed by extrapolation to zero time yields $\Phi_o\sum\mu = 10^{-5}$ cm^2/(V s).

The relative change in microwave power obtained after photoexcitation at the first absorption peak of the EDT LbL film is positive (green/blue) at all frequencies; see Figure 4B. This implies that photoexcitation leads to a real photoconductance due to mobile charge carriers that move in phase with the oscillating microwave field. A real photoconductance was also found for the soaked and EDA LbL grown films (data not shown).

The transition from predominantly imaginary to predominantly real conductivity can be explained in two ways. (1) The yield of free carriers Φ_o increases in the LbL and soaked films due to enhanced wave function delocalization. This results in more free charges and fewer excitons, increasing the real component and decreasing the imaginary component of the conductivity. Alternatively, (2) the charge carrier mobility is much higher in the LbL and soaked films, resulting in an enhanced real mobility that dominates over the imaginary component.

In what follows, the real photoconductance, obtained from the relative change in microwave power at the resonance frequency, is considered.

Figure 5 shows the wavelength dependence of the maximum in the photoconductance, ΔG_o (see section 2.5), normalized to the laser pump fluence, i.e., the photoaction spectrum. The photoaction spectrum closely follows the absorption spectrum, which means that the quantum yield for charge carrier photogeneration is independent of photon energy.

The photoexcitation density, or the average number of photoexcitations per QD, can be varied by adjustment of the laser pump fluence. Figure 6 shows the effect of the photoexcitation density on the product of the quantum yield for charge generation and the sum of the electron and hole mobility, $\Phi_o\sum\mu$. The average number of photoexcitations per QD was obtained as $I_o\sigma$, with the absorption cross section σ from ref 26. The decrease of $\Phi_o\sum\mu$ with photoexcitation density is due to second-order decay of excitons and/or charges at times shorter than the 18 ns response time of the microwave cavity. The vertical bars in Figure 6 represent the sample-to-sample variation in the results. For low excitation density, the highest value of $\Phi_o\sum\mu = 4 \times 10^{-3}$ cm^2/(V s) was obtained for a film a LbL treated with 1,2-ethanediamine film. As discussed in section 2.5, this value is a lower limit to the sum of the electron and hole mobilities. In the case of LbL films treated with 1,2-ethanedithiol, the lower limit to the mobility was found to be 2×10^{-3} cm^2/(V s). Since the thiol is a hole trap, this mobility is due to electrons only.

The lower limit to the mobility found in the present work agrees with the highest mobility values reported in the literature, which are on the order of 10^{-2} cm^2/(V s).[9,13,14] It is worth noting that in contrast to the mobility values reported here these literature values were obtained at high carrier densities[9,13] or for films with fully inorganic ligands.[14] If it is assumed that the photoconductivity is due to electrons with a mobility of 10^{-2} cm^2/(V s), the efficiency of charge carrier formation is as high as 40% for the sample with the highest mobility. The exciton binding energy is reported to be tenths of an electronvolt for individual CdSe QDs of the size examined here,[37] and therefore, such a high quantum yield of carrier formation is not expected for isolated QDs. This implies that electronic coupling strongly reduces the exciton binding energy. On the other hand, if Φ_o is small, it implies that the mobility is comparable or higher than the highest mobilities reported.[9,13,14]

The product $\Phi_o\sum\mu$ for the soaked films was found to be about an order of magnitude higher than for the drop-casted film with bulky TOPO/HDA/TDPA ligands (data not shown). For the LbL grown films the values of $\Phi_o\sum\mu$ are higher than for the soaked films; see Figure 6. The enhanced electronic coupling between QDs in the LbL grown films, as inferred from the optical data discussed in section 3.1, likely increases the quantum yield of charge carrier photogeneration and the charge mobility.

The effect of QD cross-linking by the bifunctional capping molecules on the photoconductivity is doubtful, as a similar photoconductivity has been measured in a LbL grown film using hexylamine, a monodendate ligand. This suggests that reduction of the interparticle distance alone is responsible for the high photoconductivity, as reported before.[22]

Interestingly, at times exceeding the 18 ns response time of the microwave cavity, the decay kinetics are independent of photoexcitation density, as shown for the EDT LbL film in Figure 7. This means that the charges that are present at longer

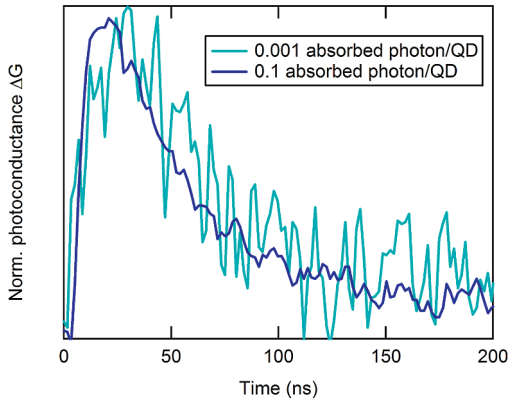

Figure 7. Normalized photoconductance transients for the EDT LbL film for different photoexcitation density.

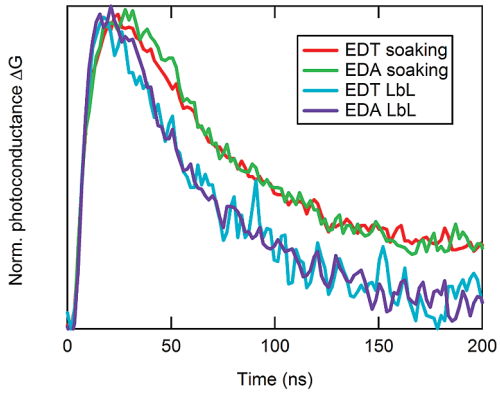

Figure 8. Normalized photoconductance of soaked and LbL grown QD films. The films were photoexcited at the first absorption peak with an excitation density of on average 0.03 absorbed photons per QD.

times predominantly decay by geminate recombination with their sibling counter charge or that the charge mobility deceases over time by relaxation at sites with lower energy or by deep trapping.

Time-resolved photoluminescence measurements (not shown) only exhibited fast (<2 ns) photoluminescence decay in the LbL films, on a time scale much shorter than the photoconductivity decay. Hence, there is no sign of (radiative) geminate recombination, suggesting that carrier trapping causes the decay of the photoconductivity. However, since the number of charges that undergo radiative geminate recombination may be low (e.g., if the carrier generation efficiency is small), this does not fully exclude geminate recombination as the mechanism responsible for the photoconductivity decay.

Figure 8 shows the normalized photoconductance of soaked and LbL grown QD films. For the LbL grown films the decay of the photoconductance is faster than for the soaked films, which can be understood on basis of a higher charge mobility in LbL grown films, leading to faster geminate recombination or charge trapping. The higher mobility for the LbL grown films agrees with the stronger electronic coupling between QDs inferred from the optical data discussed in section 3.1.

The decay kinetics are the same for films with EDT and EDA capping molecules. Since holes are surface trapped in the case of EDT capping molecules, this observation suggests that electrons dominate the photoconductivity for both capping molecules, either because they have a much higher mobility or because holes are trapped on a much shorter time scale. In this case, the decay of the photoconductivity is due to trapping of electrons with an identical rate in EDA and EDT films. For instance, shallow trapping of mobile electrons in the bigger QDs could result in identical decay dynamics in the films with different capping. However, it cannot be fully excluded that the decay of charges is due to geminate recombination, which has a similar rate in the two films, even though the holes are trapped on the surface in the case of the EDT-treated films.

4. Conclusions

Highly photoconductive films of CdSe nanocrystals have been prepared by exchanging the original bulky ligands by smaller molecules. Different methods to achieve this exchange, i.e., soaking of drop-casted films or LbL deposition, have been compared in detail. Replacement of the bulky surface ligands by EDT or EDA molecules strongly affects the optical and conductive properties. In simple drop-casted films the conductivity is mainly imaginary and dominated by the polarizability of photogenerated excitons, while introduction of EDA or EDT results in a dominant real component of the conductivity, as a result of interparticle transport of free charge carriers.

In general it is found that the LbL method is superior to the soaking approach. The LbL films exhibit (1) stronger electronic coupling, evidenced by a strong red-shift of the absorption spectrum; (2) less disorder, evidenced by the absence of broadening of the absorption features; (3) full quenching of the photoluminescence, attributed to a higher exciton diffusion coefficient and more efficient charge separation; and (4) a higher photoconductivity, as determined using the time-resolved microwave conductivity technique. The high photoconductivity is found not to be related to QD cross-linking but likely to reduction of the interparticle particle spacing. Introduction of a hole trap on the surface of the QD does not significantly influence the photoconductivity and the mobile charge decay kinetics. The product of the charge carrier generation yield and the mobility in one of the LbL grown films with EDA capping molecules was 4×10^{-3} cm^2/(V s). This implies a surprisingly high quantum yield of free charge carrier formation or a charge carrier mobility that is comparable or higher than previously reported values.

Acknowledgment. This work is part of SELECT—Silicon Based Superlattices with Spectrum Selective Absorbers. SELECT is financed by SenterNovem; program: 'Energie Onderzoek Subsidie: Lange Termijn'. The 3TU Centre for Sustainable Energy Technologies (Federation of the three Universities of Technology) is acknowledged for financial support.

References and Notes

(1) Alivisatos, A. P. *J. Phys. Chem.* **1996**, *100*, 13226.
(2) Hillhouse, H. W.; Beard, M. C. *Curr. Opin. Colloid Interface Sci.* **2009**, *14*, 245.
(3) Vanmaekelbergh, D.; Liljeroth, P. *Chem. Soc. Rev.* **2005**, *34*, 299.
(4) Dabbousi, B. O.; RodriguezViejo, J.; Mikulec, F. V.; Heine, J. R.; Mattoussi, H.; Ober, R.; Jensen, K. F.; Bawendi, M. G. *J. Phys. Chem. B* **1997**, *101*, 9463.
(5) Luther, J. M.; Beard, M. C.; Song, Q.; Law, M.; Ellingson, R. J.; Nozik, A. J. *Nano Lett.* **2007**, *7*, 1779.
(6) Trinh, M. T.; Houtepen, A. J.; Schins, J. M.; Hanrath, T.; Piris, J.; Knulst, W.; Goossens, A.; Siebbeles, L. D. A. *Nano Lett.* **2008**, *8*, 1713.
(7) Donega, C. D.; Liljeroth, P.; Vanmaekelbergh, D. *Small* **2005**, *1*, 1152.
(8) Talapin, D. V.; Murray, C. B. *Science* **2005**, *310*, 86.
(9) Yu, D.; Wehrenberg, B. L.; Jha, P.; Ma, J.; Guyot-Sionnest, P. *J. Appl. Phys.* **2006**, *99*, 104315.
(10) Koole, R.; Liljeroth, P.; Donega, C. D.; Vanmaekelbergh, D.; Meijerink, A. *J. Am. Chem. Soc.* **2006**, *128*, 10436.
(11) Luther, J. M.; Law, M.; Beard, M. C.; Song, Q.; Reese, M. O.; Ellingson, R. J.; Nozik, A. J. *Nano Lett.* **2008**, *8*, 3488.
(12) Murphy, J. E.; Beard, M. C.; Nozik, A. J. *J. Phys. Chem. B* **2006**, *110*, 25455.
(13) Yu, D.; Wang, C.; Guyot-Sionnest, P. *Science* **2003**, *300*, 1277.

(14) Kovalenko, M. V.; Scheele, M.; Talapin, D. V. *Science* **2009**, *324*, 1417.
(15) Loef, R.; Houtepen, A. J.; Talgorn, E.; Schoonman, J.; Goossens, A. *Nano Lett* **2009**, *9*, 856.
(16) Houtepen, A. J.; Kockmann, D.; Vanmaekelbergh, D. *Nano Lett.* **2008**, *8*, 3516.
(17) Guyot-Sionnest, P.; Wang, C. *J. Phys. Chem. B* **2003**, *107*, 7355.
(18) Jarosz, M. V.; Porter, V. J.; Fisher, B. R.; Kastner, M. A.; Bawendi, M. G. *Phys. Rev. B* **2004**, *70*, 195327.
(19) Klem, E. J. D.; Shukla, H.; Hinds, S.; MacNeil, D. D.; Levina, L.; Sargent, E. H. *Appl. Phys. Lett.* **2008**, *92*, 212105.
(20) Porter, V. J.; Geyer, S.; Halpert, J. E.; Kastner, M. A.; Bawendi, M. G. *J. Phys. Chem. C* **2008**, *112*, 2308.
(21) Weiss, E. A.; Chiechi, R. C.; Geyer, S. M.; Porter, V. J.; Bell, D. C.; Bawendi, M. G.; Whitesides, G. M. *J. Am. Chem. Soc.* **2008**, *130*, 74.
(22) Luther, J. M.; Law, M.; Song, Q.; Perkins, C. L.; Beard, M. C.; Nozik, A. J. *ACS Nano* **2008**, *2*, 271.
(23) Wuister, S. F.; Donega, C. D.; Meijerink, A. *J. Phys. Chem. B* **2004**, *108*, 17393.
(24) Kroeze, J. E.; Savenije, T. J.; Vermeulen, M. J. W.; Warman, J. M. *J. Phys. Chem. B* **2003**, *107*, 7696.
(25) Mekis, I.; Talapin, D. V.; Kornowski, A.; Haase, M.; Weller, H. *J. Phys. Chem. B* **2003**, *107*, 7454.
(26) Yu, W. W.; Qu, L. H.; Guo, W. Z.; Peng, X. G. *Chem. Mater.* **2003**, *15*, 2854.
(27) Wuister, S. F.; Swart, I.; van Driel, F.; Hickey, S. G.; Donega, C. D. *Nano Lett.* **2003**, *3*, 503.
(28) Kroeze, J. E.; Savenije, T. J.; Warman, J. M. *J. Am. Chem. Soc.* **2004**, *126*, 7608.
(29) Schins, J. M. P., P.; Grozema, F. C.; Abellon, R. D.; de Haas, M. P.; Siebbeles, L. D. A. *Rev. Sci. Instrum.* **2005**, *76*, 084703.
(30) Savenije, T. J.; de Haas, M. P.; Warman, J. M. *Z. Phys. Chem.—Int. J. Res. Phys. Chem. Chem. Phys.* **1999**, *212*, 201.
(31) Murray, C. B.; Norris, D. J.; Bawendi, M. G. *J. Am. Chem. Soc.* **1993**, *115*, 8706.
(32) Koole, R.; Luigjes, B.; Tachiya, M.; Pool, R.; Vlugt, T. J. H.; Donega, C. D. M.; Meijerink, A.; Vanmaekelbergh, D. *J. Phys. Chem. C* **2007**, *111*, 11208.
(33) Artemyev, M. V.; Woggon, U.; Jaschinski, H.; Gurinovich, L. I.; Gaponenko, S. V. *J. Phys. Chem. B* **2000**, *104*, 11617.
(34) Guyot-Sionnest, P.; Wehrenberg, B.; Yu, D. *J. Chem. Phys.* **2005**, *123*, 074709.
(35) Munro, A. M.; Jen-La Plante, I.; Ng, M. S.; Ginger, D. S. *J. Phys. Chem. C* **2007**, *111*, 6220.
(36) Kagan, C. R.; Murray, C. B.; Nirmal, M.; Bawendi, M. G. *Phys. Rev. Lett.* **1996**, *76*, 1517.
(37) Meulenberg, R. W.; Lee, J. R. I.; Wolcott, A.; Zhang, J. Z.; Terminello, L. J.; van Buuren, T. *ACS Nano* **2009**, *3*, 325.

JP9109546